Stable Underlying Equations for Constrained Hamiltonian Systems

Werner M. Seiler*

[1] Interdisziplinäres Zentrum für Wissenschaftliches Rechnen, Universität Heidelberg, 69120 Heidelberg, Germany

Key words Hamiltonian system, constraint, impetus-striction, stability, differential algebraic equation, numerical integration, projection method.
MSC (2000) 70H45, 37J25, 37M05

Constrained Hamiltonian systems represent a special class of differential algebraic equations appearing in many mechanical problems. We survey some possibilities for exploiting their rich geometric structures in the numerical integration of the systems. Our main theme is the construction of underlying equations for which the constraint manifold possesses good stability properties. As an application we compare position and momentum projections for systems with externally imposed holonomic constraints.

1 Introduction

Hamiltonian mechanics [14] is an old and important tool for the energy-based modelling of mechanical (and other) systems without friction. Compared with other approaches to classical mechanics like Newtonian or Lagrangian formulations, it possesses a particularly rich geometry [1]. For example, in canonical transformations positions and momenta may be transformed independently, whereas in Lagrangian mechanics the transformation of the velocities follows from the one of the positions via the chain rule. On the theoretical side, this gives us more freedom in choosing a suitable representation for a Hamiltonian systems; on the practical side, this observation is the basis of symplectic integrators [16, 26].

The modelling of larger mechanical systems almost inevitably leads to constraints. This is for example the case, if a modular approach has been taken where a larger system is broken up in smaller subsystems. Connecting the models for the subsystems yields constraints between previously independent variables. In modern theoretical physics, gauge symmetries (or gauge fixing conditions) are a natural source for constraints. If constraints are present, the true phase space in which the dynamics of the system takes place is only a subset of the originally chosen phase space. Its determination is complicated by the possible existence of further hidden constraints. Because of the constraints, one needs differential algebraic equations for the modelling (one also speaks of the descriptor form of the equations of motion). Their numerical analysis is by now fairly well understood [7, 17, 23] and a number of software packages are available.

* e-mail: werner.seiler@iwr.uni-heidelberg.de

On the true phase space the equations of motion become a standard ordinary differential equation (often called the state space form of the system) which could be integrated by any standard method. In practice, it is often impossible (or at least very expensive) to perform this reduction. An alternative is the use of an underlying equation; this is an ordinary differential equation defined on the whole phase space which coincides on the true phase space with the state space form. Such underlying equations are usually not difficult to obtain.

The simplest approach to solve a differential algebraic equation consists of integrating an underlying equation. It has the advantage that standard methods for ordinary differential equations can be applied, but it suffers potentially from a drift off from the true phase space due to numerical errors. This drift may be considered as a stability problem: the basic question is whether the constraint manifold is attractive or repulsive for the underlying equation.

There are two fundamental strategies to tackle this problem. Stabilisation techniques try to find an underlying equation for which the true phase space is at least not repulsive. Alternatively, one designs special numerical methods ensuring that the approximate solution satisfies the constraints (or at least some of them). Typically, this involves (at least implicitly) some form of projections on the true phase space.

The two strategies should be considered as complementary. Even if one uses special integrators preserving the constraints, the obtained results will benefit from a more stable formulation of the equations of motion. First of all, if the constraint manifold is attractive, less projections are needed reducing the computational effort. Secondly, while projections obviously ensure the preservation of the constraints, it is not guaranteed that the projected point is close to the true trajectory: the shorter the distance over which one must project, the smaller the errors introduced that way.

The main theme of this article is to show that various physically motivated formulations of the equations of motion of a constrained Hamiltonian system may be understood as stabilisation techniques, although the original motivations of their derivation were often completely different problems like quantisation. More precisely, we will first study the classical Dirac theory of constrained Hamiltonian systems [11, 12] which has been applied for the numerical integration of the systems in [20, 31]. Then we turn our attention to the impetus-striction formalism. It was introduced under this name by Dichmann et al. [9, 10, 22] mainly for field theories and appeared independently at several other places [19, 25, 33] in the context of the numerical analysis of mechanical systems. We will present a new purely Hamiltonian point of view of it as a canonical momentum projection.

As an application of these results, we compare the effect of position and momentum projections. In systems with externally imposed constraints the momentum constraints are hidden. For this reason, they are often neglected in the numerical integration and only position projections are used. However, we will show that momentum projections are not only cheaper but also more effective. While our analysis makes significant use of techniques specific to Hamiltonian systems like canonical transformations, it should be emphasised that the result holds for much larger classes of systems. Alishenas [2, 3] obtained for example identical results for Lagrangian systems using classical error analysis techniques.

This article is organised as follows. The next section reviews some basic notions from Hamiltonian mechanics which are needed later. Section 3 covers the classical Dirac theory and derives in particular the Hamilton-Dirac equations. We then specialise the results to regular systems with externally imposed constraints. Section 5 derives the impetus-striction formalism in a novel purely Hamiltonian manner showing that it consists effectively of a canonical transformation. Afterwards we discuss the interpretation of this transformation as a momentum projection. Section 7 applies the theory developed so far for a comparison of position and momentum projections. Finally, we verify our theoretical results on a simple example, namely the planar pendulum in Cartesian coordinates.

2 Hamiltonian Mechanics

The traditional starting point for the modelling of a mechanical system is not directly the Hamiltonian formulation but the Lagrangian one. Let $\boldsymbol{q}$ be (generalised) coordinates in an N-dimensional configuration space $\mathcal{Q}$. We restrict our presentation to autonomous systems, as explicit time dependencies can always be treated by considering the time as additional coordinate in an extended configuration space. The Lagrangian is then a real-valued function $L(\boldsymbol{q}, \dot{\boldsymbol{q}})$ on the tangent bundle $T\mathcal{Q}$ and the dynamics of a mechanical system described by it are given by the well-known *Euler-Lagrange equations*

$$\frac{d}{dt}\left(\frac{\partial L}{\partial \dot{\boldsymbol{q}}}\right) - \frac{\partial L}{\partial \boldsymbol{q}} = 0\,. \tag{1}$$

The Lagrangian L is called regular, if the Hessian $\frac{\partial^2 L}{\partial \dot{\boldsymbol{q}} \partial \dot{\boldsymbol{q}}}$ with respect to the velocities $\dot{\boldsymbol{q}}$ is regular. In this case all equations in (1) are second order.

The most important case for applications are *natural systems*. Here $\mathcal{Q}$ is a Riemannian manifold, i. e. we are in addition given a scalar product on $T\mathcal{Q}$. The scalar product is defined by a symmetric, positive definite matrix function $M(\boldsymbol{q})$ and for vector $\boldsymbol{u}, \boldsymbol{v} \in T_{\boldsymbol{q}}\mathcal{Q}$ we have $(\boldsymbol{u}, \boldsymbol{v})_M = \boldsymbol{u}^t M(\boldsymbol{q})\boldsymbol{v}$. For a natural mechanical system, M is the mass matrix and the Lagrangian is of the form $L(\boldsymbol{q}, \dot{\boldsymbol{q}}) = \frac{1}{2}(\dot{\boldsymbol{q}}, \dot{\boldsymbol{q}})_M - V(\boldsymbol{q})$ with some real valued potential V. For a constant mass matrix, (1) leads then to the familiar Newtonian equations $M\ddot{\boldsymbol{q}} = -\partial V/\partial \boldsymbol{q}$.

The Hamiltonian formulation is obtained via a *Legendre transformation*. Geometrically, it is given by the fibre derivative of L and maps the tangent bundle $T\mathcal{Q}$ into the cotangent bundle $T^*\mathcal{Q}$, the phase space of Hamiltonian mechanics. In coordinates, we introduce the canonically conjugate momenta

$$\boldsymbol{p} = \frac{\partial L}{\partial \dot{\boldsymbol{q}}}(\boldsymbol{q}, \dot{\boldsymbol{q}})\,. \tag{2}$$

In the case of a natural system, this leads to the familiar expression $\boldsymbol{p} = M\dot{\boldsymbol{q}}$. For a regular Lagrangian, (2) may be inverted and the velocities $\dot{\boldsymbol{q}}$ can be expressed as functions of $(\boldsymbol{q}, \boldsymbol{p})$. The *canonical Hamiltonian* of the system given by $H_c = \boldsymbol{p}^t\dot{\boldsymbol{q}} - L(\boldsymbol{q}, \dot{\boldsymbol{q}})$ is then a real-valued functions of $T^*\mathcal{Q}$ and represents physically the total energy of the system.

The Hamiltonian equations of motion are obtained by entering the momenta into (1):

$$\dot{\boldsymbol{q}} = \frac{\partial H_c}{\partial \boldsymbol{p}}\,, \qquad \dot{\boldsymbol{p}} = -\frac{\partial H_c}{\partial \boldsymbol{q}}\,. \tag{3}$$

A convenient way to express these equations is provided by the *Poisson bracket*. If $F(\boldsymbol{q}, \boldsymbol{p})$, $G(\boldsymbol{q}, \boldsymbol{p})$ are two arbitrary observables, i. e. real-valued functions on $T^*\mathcal{Q}$, then we define

$$\{F, G\} = \left(\frac{\partial F}{\partial \boldsymbol{q}}\right)^t \frac{\partial G}{\partial \boldsymbol{p}} - \left(\frac{\partial G}{\partial \boldsymbol{q}}\right)^t \frac{\partial F}{\partial \boldsymbol{p}}\,. \tag{4}$$

This bracket is linear in its arguments, skew-symmetric $\{F,G\} = -\{G,F\}$ and satisfies the Jacobi identity $\{F,\{G,H\}\} + \{G,\{H,F\}\} + \{H,\{F,G\}\} = 0$. The equations of motion (3) may now be concisely written in the form

$$\dot{\boldsymbol{q}} = \{\boldsymbol{q}, H_c\}\,, \qquad \dot{\boldsymbol{p}} = \{\boldsymbol{p}, H_c\}\,. \tag{5}$$

More generally, the evolution of any observable along trajectories of the Hamiltonian system (3) is determined by $\dot{F} = \{F, H_c\}$, as one can easily check. Note that this trivially implies energy conservation, as $\dot{H}_c = \{H_c, H_c\} = 0$.

Poisson brackets are also useful for characterising *canonical transformations*. These are coordinate transformations $(\boldsymbol{q},\boldsymbol{p}) \leftrightarrow (\boldsymbol{Q},\boldsymbol{P})$ that preserve the brackets. They may be derived with the help of *generating functions* [14, Chapt. VIII]. Different types of generating functions exist; we will use functions $S(\boldsymbol{Q},\boldsymbol{p})$. The corresponding canonical transformation is then implicitly defined by the equations

$$\boldsymbol{q} = \frac{\partial S}{\partial \boldsymbol{p}}(\boldsymbol{Q},\boldsymbol{p})\,, \qquad \boldsymbol{P} = \frac{\partial S}{\partial \boldsymbol{Q}}(\boldsymbol{Q},\boldsymbol{p})\,. \tag{6}$$

3 Dirac Theory of Constrained Hamiltonian Systems

The Dirac theory considers the case that the relations (2) cannot be solved for all velocities $\dot{\boldsymbol{q}}$. Obviously, this only happens, if the Hessian $\frac{\partial^2 L}{\partial\dot{\boldsymbol{q}}\partial\dot{\boldsymbol{q}}}$ does not possess full rank. By elimination, we obtain then from (2) some *primary constraints*

$$\boldsymbol{\phi}(\boldsymbol{q},\boldsymbol{p}) = 0\,. \tag{7}$$

We will always assume that these are irreducible, i. e. that their Jacobian has maximal rank. Their number is then determined by the rank defect of the Hessian $\frac{\partial^2 L}{\partial\dot{\boldsymbol{q}}\partial\dot{\boldsymbol{q}}}$. The meaning of the constraints is that the dynamics does not use the whole phase space but at most the submanifold described by (7).

For an unconstrained system it was obvious that the canonical Hamiltonian H_c is a function of $(\boldsymbol{q},\boldsymbol{p})$ only, since the velocity $\dot{\boldsymbol{q}}$ can be eliminated using (2). Due to the special form of H_c, this is also possible in a constrained system, but the resulting function H_c is uniquely defined only *on* the constraint manifold. Thus the formalism remains unchanged, if we add an arbitrary linear combination[1] of the constraint functions $\boldsymbol{\phi}$. This leads to the *total Hamiltonian* $H_t(\boldsymbol{q},\boldsymbol{p}) = H_c + \boldsymbol{u}^t\boldsymbol{\phi}$ where the multipliers $\boldsymbol{u}$ are a priori arbitrary functions of $(\boldsymbol{q},\boldsymbol{p})$.

Using constrained variational calculus, one can show that the Euler-Lagrange equations (1) are equivalent to the following first order system

$$\dot{\boldsymbol{q}} = \frac{\partial H_c}{\partial \boldsymbol{p}} + \boldsymbol{u}^t\frac{\partial \boldsymbol{\phi}}{\partial \boldsymbol{p}}\,, \qquad \dot{\boldsymbol{p}} = -\frac{\partial H_c}{\partial \boldsymbol{q}} - \boldsymbol{u}^t\frac{\partial \boldsymbol{\phi}}{\partial \boldsymbol{q}}\,, \qquad \boldsymbol{\phi} = 0\,. \tag{8}$$

It represents the traditional starting point for a numerical integration. Its differential part defines an underlying equation which, however, is not Hamiltonian. By contrast, the differential part of the system

$$\dot{\boldsymbol{q}} = \{\boldsymbol{q}, H_t\}\,, \qquad \dot{\boldsymbol{p}} = \{\boldsymbol{p}, H_t\}\,, \qquad \boldsymbol{\phi} = 0\,, \tag{9}$$

[1] Here and in the sequel the coefficients of "linear combinations" are allowed to be arbitrary functions of the phase space variables $(\boldsymbol{q},\boldsymbol{p})$.

is Hamiltonian. The two systems are equivalent, as their right hand sides differ only by linear combinations of the constraint functions. More generally, the time evolution of any phase space function $F(\boldsymbol{q}, \boldsymbol{p})$ can be written as $\dot{F} = \{F, H_t\}$.

In a consistent theory, the constraints $\boldsymbol{\phi} = 0$ must be preserved by the evolution of the system. This leads to the conditions $\dot{\boldsymbol{\phi}} = \{\boldsymbol{\phi}, H_t\} \approx 0$. The $\approx$ signals a *weak equality*; it may hold only after taking the constraints into account. By a standard argument in differential geometry, this implies that the Poisson bracket $\{\boldsymbol{\phi}, H_t\}$ must be a linear combination of the constraint functions. There are three possibilities: (i) it yields modulo the constraints an equation of the form $1 = 0$; (ii) it becomes $0 = 0$; (iii) we obtain a new equation $\psi(\boldsymbol{q}, \boldsymbol{p}) = 0$.

(i) implies inconsistent equations of motion; they do not possess any solution. (ii) is the desired outcome. (iii) splits into two sub-cases. If the function ψ depends on some of the multipliers $\boldsymbol{u}$, we consider it as an equation determining one of them.[2] Otherwise we have a *secondary constraint*. We must then check whether all secondary constraints are preserved by repeating the procedure until we either encounter case (i) or all constraints lead to case (ii). This is the famous *Dirac algorithm*, a special version of the general completion procedure for differential algebraic equations [30, 32].

Let $\boldsymbol{\chi}$ denote all K constraint functions of the systems: the primary ones and those obtained with the Dirac algorithm. They can be divided into two classes by studying the $K \times K$ matrix of their Poisson brackets $C = \{\boldsymbol{\chi}, \boldsymbol{\chi}\}$. As C is skew-symmetric, its rank M is even. Let us assume for simplicity that after a simple relabelling of the entries of $\boldsymbol{\chi}$ the top left $M \times M$ sub-matrix of C is regular (in general we must redefine the constraint functions by taking linear combinations to achieve this). Then we call the constraint functions $\chi_1, \dots, \chi_M$ *second class*. The Poisson bracket of a *first class* constraint function ψ with any other constraint function χ (primary or higher) vanishes weakly: $\{\psi, \boldsymbol{\chi}\} \approx 0$. In our case the constraint functions $\chi_{M+1}, \dots, \chi_K$ are first class. Obviously this classification can be performed only after *all* constraints have been found.

First class constraints generate gauge symmetries [18] and lead to arbitrary functions in the general solution of the equations of motion; these are under-determined [32]. In the sequel we will always assume that no first class constraints are present. This is no real restriction, as they appear very rarely in finite-dimensional systems. Furthermore they can always be transformed into second class constraints by a gauge fixing, i. e. by adding further constraints removing the under-determinacy.

Second class constraints signal the presence of unphysical or redundant degrees of freedom; as mentioned above their number M is always even. If there are no first class constraints, the matrix C is regular (otherwise we take the sub-matrix of C corresponding to the second class constraint functions) and we introduce the *Dirac bracket* of two observables F, G as

$$\{F, G\}^* = \{F, G\} - \big(\{F, \boldsymbol{\chi}\}\big)^t C^{-1} \{\boldsymbol{\chi}, G\}\,. \tag{10}$$

The Dirac bracket possesses exactly the same algebraic properties as the canonical Poisson bracket (4): it is linear, skew-symmetric and satisfies the Jacobi identity.

Consider for any observable $F(\boldsymbol{q}, \boldsymbol{p})$ the dynamics defined by $\dot{F} = \{F, H_c\}^*$. We prove in two steps that for initial data on the constraint manifold these dynamics are equivalent to the original ones defined by the total Hamiltonian and the standard Poisson bracket. It suffices to

[2] Note that as these are weak equations they determine the multipliers only up to linear combinations of the constraint functions.

show that the right hand sides of the respective equations of motions are weakly equal, as for such initial data the trajectories never leave the constraint manifold. As first step we note that for the Dirac bracket it makes no difference whether H_t or H_c is used:

$$\begin{aligned}\{F,H_t\}^* &= \{F,H_t\} - \big(\{F,\boldsymbol{\chi}\}\big)^t C^{-1}\{\boldsymbol{\chi},H_t\}\\ &\approx \{F,H_c\} - \big(\{F,\boldsymbol{\chi}\}\big)^t C^{-1}\{\boldsymbol{\chi},H_c\} + \boldsymbol{u}^t\Big(\{F,\boldsymbol{\chi}\} - \big(\{F,\boldsymbol{\chi}\}\big)^t C^{-1}\{\boldsymbol{\chi},\boldsymbol{\chi}\}\Big)\\ &= \{F,H_c\}^*\,.\end{aligned} \tag{11}$$

Here we used in the second line that all Poisson brackets involving the multipliers $\boldsymbol{u}$ are multiplied by constraint functions and in the last line the definition of C. As second step we show that on the constraint manifold Dirac and Poisson bracket generate the same dynamics with the total Hamiltonian H_t:

$$\{F,H_t\}^* = \{F,H_t\} - \big(\{F,\boldsymbol{\chi}\}\big)^t C^{-1}\{\boldsymbol{\chi},H_t\} \approx \{F,H_t\}\,, \tag{12}$$

as after the completion of the Dirac algorithm $\{\boldsymbol{\chi},H_t\}$ is a linear combination of constraint functions. We are thus lead to the *Hamilton-Dirac equations*[3]

$$\dot{\boldsymbol{q}} = \{\boldsymbol{q},H_c\}^*\,,\qquad \dot{\boldsymbol{p}} = \{\boldsymbol{p},H_c\}^*\,. \tag{13}$$

The Dirac bracket effectively eliminates the second class constraints, as they become *distinguished* or *Casimir functions:* the Dirac bracket of any phase space function F with a second class constraint function vanishes, as again by the definition of C

$$\{F,\boldsymbol{\chi}\}^* = \{F,\boldsymbol{\chi}\} - \big(\{F,\boldsymbol{\chi}\}\big)^t C^{-1}\{\boldsymbol{\chi},\boldsymbol{\chi}\} = 0\,. \tag{14}$$

Note that this is a strong and not only a weak equality! Historically, this observation was Dirac's motivation for introducing his bracket, as it allows for a consistent quantisation of constrained systems.

In our context, its importance lies in the fact that it implies that in most relevant cases the constraint manifold is orbitally stable[4] for the flow of the Hamilton-Dirac equations (13). The constraint functions $\boldsymbol{\chi}$ foliate the phase space into disjoint submanifolds $\mathcal{M}_{\boldsymbol{\epsilon}}$ defined by $\boldsymbol{\chi}(\boldsymbol{q},\boldsymbol{p}) = \boldsymbol{\epsilon}$ with constants $\boldsymbol{\epsilon}$. Exact solutions of the Hamilton-Dirac equations (13) lie completely on the submanifold $\mathcal{M}_{\boldsymbol{\epsilon}}$ determined by the initial data. The equations do not "see" the values $\boldsymbol{\epsilon}$; in particular $\boldsymbol{\epsilon} = 0$ is not distinguished. This is a trivial consequence of the fact that the Dirac bracket (10) depends only on the derivatives of the constraint functions and not on the functions themselves.

Numerical errors are thus neither damped nor amplified by the dynamics. They lead to different values $\bar{\boldsymbol{\epsilon}}$ and without further errors the trajectory would stay on the submanifold $\mathcal{M}_{\bar{\boldsymbol{\epsilon}}}$. If the submanifolds $\mathcal{M}_{\boldsymbol{\epsilon}}$ are compact, there exists trivially an upper bound (depending only on $\boldsymbol{\epsilon}$) for $\mathrm{dist}(\boldsymbol{z},\mathcal{M}_0)$ with $\boldsymbol{z} \in \mathcal{M}_{\boldsymbol{\epsilon}}$. The same holds for quadratic constraint functions $\boldsymbol{\chi}$. Hence in both case we have obviously orbital stability.

[3] For historical correctness one should remark that Dirac did not consider (13). He worked with the total Hamiltonian H_t instead of the canonical one H_c. But we proved above that the corresponding equations of motion are weakly equal. Computationally the use of H_c is more efficient, as it leads to simpler equations.

[4] A manifold $\mathcal{M}$ is called orbitally stable for a dynamical system $\dot{\boldsymbol{z}} = f(\boldsymbol{z})$, if for every $\epsilon > 0$ there exists a $\delta > 0$ such that for any solution $\boldsymbol{z}(t)$ satisfying $\mathrm{dist}(\boldsymbol{z}(0),\mathcal{M}) < \delta$ the inequality $\mathrm{dist}(\boldsymbol{z}(t),\mathcal{M}) < \epsilon$ holds [15].

4 Regular Systems with Externally Imposed Constraints

For applications the most important type of constrained systems is described by a regular Lagrangian L and subject to k externally imposed constraints[5] $\boldsymbol{\phi}(q) = 0$, the *position constraints*. In principle, this situation cannot be treated within the Dirac formalism, as it covers only singular Lagrangians. There exist several ways to derive the equations of motion. The simplest one introduces Lagrange multipliers $\boldsymbol{\mu}$ and considers the augmented Lagrangian $L' = L + \boldsymbol{\mu}^t\boldsymbol{\phi}$. In contrast to the multipliers $\boldsymbol{u}$ in the Dirac theory, $\boldsymbol{\mu}$ must be considered as additional dynamical variables and not as undetermined functions. Now L' is obviously singular, as it does not depend on the "velocities" $\dot{\boldsymbol{\mu}}$, and we may apply the Dirac theory.

If we denote by H the Hamiltonian for the regular system, then the classical Hamiltonian equations of motion (8) simplify now to

$$\dot{\boldsymbol{q}} = \frac{\partial H}{\partial \boldsymbol{p}}\,, \qquad \dot{\boldsymbol{p}} = -\frac{\partial H}{\partial \boldsymbol{q}} - \boldsymbol{\mu}^t\frac{\partial \boldsymbol{\phi}}{\partial \boldsymbol{q}}\,, \qquad \boldsymbol{\phi} = 0\,, \tag{15}$$

as the constraints do not depend on the momenta. Differentiation of the position constraints leads to the *momentum constraints* $\boldsymbol{\psi} = \dot{\boldsymbol{\phi}} = \{\boldsymbol{\phi}, H\} \approx 0$. Differentiation of these in turn yields a linear system of equations for the multipliers $\boldsymbol{\mu}$:

$$\{\boldsymbol{\psi}, \boldsymbol{\phi}\}\boldsymbol{\mu} \approx \{\boldsymbol{\psi}, H\}\,. \tag{16}$$

Its matrix evaluates to $(\frac{\partial \boldsymbol{\phi}}{\partial \boldsymbol{q}})^t \frac{\partial^2 H}{\partial \boldsymbol{p}\partial \boldsymbol{p}} \frac{\partial \boldsymbol{\phi}}{\partial \boldsymbol{q}}$ and thus is regular under the made assumptions. The differential part of the Hamiltonian system (9) takes the form (with the multiplier $\boldsymbol{\mu}$ again determined by (16))

$$\dot{\boldsymbol{q}} = \frac{\partial H}{\partial \boldsymbol{p}} + \frac{\partial(\boldsymbol{\mu}^t\boldsymbol{\phi})}{\partial \boldsymbol{p}}\,, \qquad \dot{\boldsymbol{p}} = -\frac{\partial H}{\partial \boldsymbol{q}} + \frac{\partial(\boldsymbol{\mu}^t\boldsymbol{\phi})}{\partial \boldsymbol{q}} \tag{17}$$

and differs from (15) only by terms proportional to the position constraints functions $\boldsymbol{\phi}$.

For the Dirac formalism, we introduce canonically conjugate momenta $\boldsymbol{\pi}$ for the additional variables $\boldsymbol{\mu}$. The primary constraints are $\boldsymbol{\pi} = 0$. If we denote by H the Hamiltonian for the regular system, the canonical Hamiltonian of the constrained system is $H_c = H - \boldsymbol{\mu}^t\boldsymbol{\phi}$; the total one is $H_t = H_c + \boldsymbol{u}^t\boldsymbol{\pi}$. The Dirac algorithm yields as secondary constraints $\boldsymbol{\phi} = 0$ and as tertiary constraints the momentum constraints $\boldsymbol{\psi} = \{\boldsymbol{\phi}, H_t\} \approx \{\boldsymbol{\phi}, H\} \approx 0$. The next step provides algebraic equations for the auxiliary variables $\boldsymbol{\mu}$:

$$\{\boldsymbol{\psi}, H\} - \boldsymbol{\mu}^t\{\boldsymbol{\psi}, \boldsymbol{\phi}\} \approx 0\,. \tag{18}$$

Obviously, they are equivalent to (16). The fifth and last step yields $\boldsymbol{u} = 0$.

The main problem in using Dirac brackets is the inversion of the matrix C of the Poisson brackets of the constraint functions. For a larger number K of constraints one can no longer do this symbolically. Thus one must numerically invert a $K \times K$ matrix at each evaluation of the equations of motion. In our special case $K = 2k$ and the matrix C can be partitioned into four $k \times k$ sub-matrices

$$C = \begin{pmatrix} 0 & Q \\ -Q^t & S \end{pmatrix} \tag{19}$$

[5] We restrict here to holonomic constraints, i. e. we do not allow that $\boldsymbol{\phi}$ depends on the velocities $\dot{\boldsymbol{q}}$. Anholonomic systems do not possess a proper Hamiltonian formulation [27].

where $Q = \{\boldsymbol{\phi}, \boldsymbol{\psi}\}$ and $S = \{\boldsymbol{\psi}, \boldsymbol{\psi}\}$. The inversion of such a matrix can be reduced to the inversion of one $k \times k$ matrix plus two matrix multiplications, as

$$C^{-1} = \begin{pmatrix} Q^{-t}SQ^{-1} & -Q^{-t} \\ Q^{-1} & 0 \end{pmatrix} . \tag{20}$$

The Hamilton-Dirac equations take now the following form:

$$\begin{aligned} \dot{\boldsymbol{q}} &= \frac{\partial H}{\partial \boldsymbol{p}} - \left(\frac{\partial \boldsymbol{\psi}}{\partial \boldsymbol{p}}\right)^t Q^{-1}\boldsymbol{\psi} , \\ \dot{\boldsymbol{p}} &= -\frac{\partial H}{\partial \boldsymbol{q}} - \left(\frac{\partial \boldsymbol{\phi}}{\partial \boldsymbol{q}}\right)^t Q^{-1}\{\boldsymbol{\psi}, H\} + \left[\left(\frac{\partial \boldsymbol{\phi}}{\partial \boldsymbol{q}}\right)^t Q^{-t}SQ^{-1} + \left(\frac{\partial \boldsymbol{\psi}}{\partial \boldsymbol{q}}\right)^t Q^{-1}\right]\boldsymbol{\psi} . \end{aligned} \tag{21}$$

Taking (16) into account, we see that they differ from the standard equations of motion (15) only by some terms multiplied by the momentum constraints functions $\boldsymbol{\psi}$. Thus both formulations are weakly equal.

5 The Impetus-Striction Formalism

An alternative approach for the treatment of regular systems with externally imposed constraints is provided by the impetus-striction formalism [9, 10, 22]. It is also based on an augmented Lagrangian, but it adds the *time derivatives* of the constraint functions and uses $L^* = L + \boldsymbol{\lambda}^t \frac{d}{dt}\boldsymbol{\phi}$ with multipliers $\boldsymbol{\lambda}$ which must again be considered as additional dynamical variables. Obviously, L^* is a singular Lagrangian, too, and we can straightforwardly apply the Dirac theory.

This approach represents a special case of *vakonomic mechanics* [4]. Its fundamental axiom is that the equations of motion of a constrained system are always of a variational nature – even if one considers anholonomic constraints $\boldsymbol{\psi}(\boldsymbol{q}, \dot{\boldsymbol{q}}) = 0$. The calculus of variations leads then to adding the constraint functions with multipliers to the regular Lagrangian. However, the vakonomic equations of motion are generally not equivalent to those derived with the Principle of d'Alembert. Experiments seem to indicate that they do not correctly describe the physical reality [21].

In our special case of differentiated holonomic constraints, i. e. $\boldsymbol{\psi} = \dot{\boldsymbol{\phi}}$, the two Lagrangians L' and L^* are equivalent, as they differ only by a total derivative upon the identification $\boldsymbol{\mu} = -d\boldsymbol{\lambda}/dt$. Thus both yield the same Euler-Lagrange equations. But the Legendre transformations differ and the canonically conjugate momenta for L^* and L' are related by

$$\boldsymbol{p}^* = \frac{\partial L^*}{\partial \dot{\boldsymbol{q}}} = \boldsymbol{p} + \boldsymbol{\lambda}^t \frac{\partial \boldsymbol{\phi}}{\partial \boldsymbol{q}} . \tag{22}$$

The standard approach to the impetus-striction formalism consists of first defining a pre-Hamiltonian $\tilde{H}^*$ in which $\boldsymbol{\lambda}$ is still treated as a parameter. Then $\boldsymbol{\lambda}$ is determined by requiring that $\dot{\boldsymbol{\phi}} = \{\boldsymbol{\phi}, \tilde{H}^*\} = 0$ (or alternatively by a minimisation principle [10]). The thus obtained values for $\boldsymbol{\lambda}$ are called *strictions* and entering them into (22) defines the *impetuses* $\boldsymbol{p}^*$. Entering the strictions into the pre-Hamiltonian $\tilde{H}^*$ yields the Hamiltonian H^* and one can show that the corresponding Hamiltonian equations of motion

$$\dot{\boldsymbol{q}} = \{\boldsymbol{q}, H^*\} , \qquad \dot{\boldsymbol{p}}^* = \{\boldsymbol{p}^*, H^*\} \tag{23}$$

form an underlying equation for the constrained system. Similar to our considerations in the last section, one may view the impetus-striction formalism as a short cut to the full Dirac analysis of the singular Lagrangian L^* (see [28] for more details).

We present now a new purely Hamiltonian derivation of the impetus-striction formalism interpreting (22) as part of a canonical transformation. As starting point we take this time a regular Hamiltonian $H(\boldsymbol{q},\boldsymbol{p})$, i.e. we assume that its Hessian $\frac{\partial^2 H}{\partial \boldsymbol{p}\partial \boldsymbol{p}}$ with respect to the momenta is regular, and impose some (irreducible) position constraints $\boldsymbol{\phi}(\boldsymbol{q}) = 0$.

We consider the canonical transformation $(\boldsymbol{q},\boldsymbol{p}) \leftrightarrow (\boldsymbol{q}^*,\boldsymbol{p}^*)$ defined by the generating function $S(\boldsymbol{q},\boldsymbol{p}^*) = \boldsymbol{q}^t\boldsymbol{p}^* - \big(\boldsymbol{\lambda}(\boldsymbol{q},\boldsymbol{p}^*)\big)^t\boldsymbol{\phi}(\boldsymbol{q})$ where $\boldsymbol{\lambda}(\boldsymbol{q},\boldsymbol{p}^*)$ are yet arbitrary functions. It has the form

$$\begin{aligned} \boldsymbol{q}^* &= \boldsymbol{q} - \left(\frac{\partial\boldsymbol{\lambda}}{\partial\boldsymbol{p}^*}(\boldsymbol{q},\boldsymbol{p}^*)\right)^t \boldsymbol{\phi}(\boldsymbol{q})\,, \\ \boldsymbol{p} &= \boldsymbol{p}^* - \left(\frac{\partial\boldsymbol{\lambda}}{\partial\boldsymbol{q}}(\boldsymbol{q},\boldsymbol{p}^*)\right)^t \boldsymbol{\phi}(\boldsymbol{q}) - \big(\boldsymbol{\lambda}(\boldsymbol{q},\boldsymbol{p}^*)\big)^t\frac{\partial\boldsymbol{\phi}}{\partial\boldsymbol{q}}(\boldsymbol{q})\,. \end{aligned} \tag{24}$$

We determine the functions $\boldsymbol{\lambda}$ by demanding that for any point $(\boldsymbol{q}^*,\boldsymbol{p}^*)$ on the primary constraint manifold $\mathcal{M}_1$ defined by $\boldsymbol{\phi}(\boldsymbol{q}^*) = 0$ the transformed point $(\boldsymbol{q},\boldsymbol{p})$ lies on the secondary constraint manifold $\mathcal{M}_2$ defined by $\boldsymbol{\phi}(\boldsymbol{q}) = 0$ *and* $\boldsymbol{\psi}(\boldsymbol{q},\boldsymbol{p}) = 0$ where again $\boldsymbol{\psi} = \{\boldsymbol{\phi}, H\}$ are the momentum constraint functions. Thus we want to consider (24) as a kind of symplectic projection on the true phase space $\mathcal{M}_2$. This condition is equivalent to

$$\Big(\frac{\partial\boldsymbol{\phi}}{\partial\boldsymbol{q}}(\boldsymbol{q})\Big)^t\frac{\partial H}{\partial\boldsymbol{p}}\Big(\boldsymbol{q},\boldsymbol{p}^* - \big(\boldsymbol{\lambda}(\boldsymbol{q},\boldsymbol{p}^*)\big)^t\frac{\partial\boldsymbol{\phi}}{\partial\boldsymbol{q}}(\boldsymbol{q})\Big) = 0 \tag{25}$$

and its solution $\boldsymbol{\lambda}$ are the strictions.

Restricted to the primary constraint manifold $\mathcal{M}_1$ the canonical transformation (24) simplifies considerably, as the constraint functions $\boldsymbol{\phi}$ vanish, and we obtain

$$\boldsymbol{q}^* = \boldsymbol{q}\,, \qquad \boldsymbol{p} = \boldsymbol{p}^* - \boldsymbol{\lambda}^t(\boldsymbol{q},\boldsymbol{p}^*)\frac{\partial\boldsymbol{\phi}}{\partial\boldsymbol{q}}(\boldsymbol{q}) \tag{26}$$

which is just (22). Furthermore, on $\mathcal{M}_1$ the transformed Hamiltonian is given by

$$H^*(\boldsymbol{q}^*,\boldsymbol{p}^*) = H\Big(\boldsymbol{q}^*,\boldsymbol{p}^* - \boldsymbol{\lambda}^t\frac{\partial\boldsymbol{\phi}}{\partial\boldsymbol{q}}\Big)\,. \tag{27}$$

This is the same Hamiltonian as obtained in the standard Lagrangian approach.

We claim now that the Hamiltonian equations of motion

$$\dot{\boldsymbol{q}}^* = \{\boldsymbol{q}^*, H^*\}\,, \quad \dot{\boldsymbol{p}}^* = \{\boldsymbol{p}^*, H^*\} \tag{28}$$

derived with the canonical Poisson bracket for the variables $(\boldsymbol{q}^*,\boldsymbol{p}^*)$ and the transformed Hamiltonian H^* represent an underlying differential equation for the constrained system. This assertion is not trivial, since the Poisson brackets in (28) include differentiations normal to the constraint manifold and the Hamiltonian H^* was derived with the restricted canonical transformation (26) valid only on $\mathcal{M}_1$.

Our proof is based on the Dirac theory. One possibility for the equations of motion of the constrained system are the Hamiltonian-Dirac equations (13) for $H(\boldsymbol{q}, \boldsymbol{p})$. The Dirac bracket satisfies for arbitrary phase space functions F, G [18]

$$\{F\big|_{\mathcal{M}_2}, G\big|_{\mathcal{M}_2}\} = \{F, G\}^*\big|_{\mathcal{M}_2}\,. \tag{29}$$

Thus, it does not matter whether we first restrict the functions to the true phase space $\mathcal{M}_2$ and then compute their Poisson bracket or whether we first compute their Dirac bracket and then restrict to $\mathcal{M}_2$. In this sense, the Dirac bracket can be considered as the on $\mathcal{M}_2$ by the canonical Poisson bracket induced bracket.

Since we are only interested in solutions of the equations of motion (28) living on the constraint manifold $\mathcal{M}_2$, we evaluate the Poisson brackets on the right hand side of (28) always for functions restricted to $\mathcal{M}_2$. But there H^* is just H after a canonical transformation which by definition leaves Poisson brackets invariant. Hence we may consider the right hand sides of (28) as the Poisson brackets of the canonical variables and H (both restricted to $\mathcal{M}_2$) which are by (29) just their Dirac brackets. This implies that restricted to $\mathcal{M}_2$ the equations (28) are equivalent to the equations of motion derived with the Dirac bracket. Thus solutions for initial data on $\mathcal{M}_2$ stay on $\mathcal{M}_2$ and yield trajectories of the constrained system. Furthermore every trajectory can be obtained this way and (28) represents an underlying Hamiltonian system.

Substituting (27) in (28) yields

$$\dot{\boldsymbol{q}}^* = \frac{\partial H}{\partial \boldsymbol{p}}\,, \qquad \dot{\boldsymbol{p}}^* = -\frac{\partial H}{\partial \boldsymbol{q}} + \boldsymbol{\lambda}^t \frac{\partial^2 \boldsymbol{\phi}}{\partial \boldsymbol{q} \partial \boldsymbol{q}} \frac{\partial H}{\partial \boldsymbol{p}} \tag{30}$$

where the functions are evaluated at $(\boldsymbol{q}^*, \boldsymbol{p}^* - \boldsymbol{\lambda}^t \frac{\partial \boldsymbol{\phi}}{\partial \boldsymbol{q}})$. All terms containing derivatives of the strictions $\boldsymbol{\lambda}$ disappear because of the defining equation (25). This is important for the numerical integration, as it implies that numerical values for $\boldsymbol{\lambda}$ suffice. The second term in the equation for $\dot{\boldsymbol{p}}^*$ represents the constraint forces. An important difference in comparison with other approaches is that they depend on the second derivatives of the constraint functions $\boldsymbol{\phi}$ whereas usually only first derivatives appear.

Similar to our results for the Hamilton-Dirac equations (13), we can easily conclude from these considerations that the submanifolds $\mathcal{M}_{\boldsymbol{\epsilon}}$ defined by $\boldsymbol{\phi}(\boldsymbol{q}) = \boldsymbol{\epsilon}$ with constants $\boldsymbol{\epsilon}$ are orbitally stable, if they are compact. Again the crucial point is that in (30) only derivatives of the position constraint functions $\boldsymbol{\phi}$ appear and that $\mathcal{M}_{\boldsymbol{\epsilon}}$ is an invariant manifold for the flow.

If we apply the Dirac theory to the Hamiltonian H^* and the constraint functions $\boldsymbol{\phi}$, then by definition of the strictions $\{\boldsymbol{\phi}, H^*\} = 0$. Thus no secondary constraints appear and the position constraints are first integrals. Since the Poisson brackets $\{\boldsymbol{\phi}, \boldsymbol{\phi}\}$ trivially vanish, they are first class and thus related to gauge symmetries. The gauge transformation generated by an arbitrary linear combination $\boldsymbol{\epsilon}^t \boldsymbol{\phi}$ with constant coefficients has the form

$$\delta \boldsymbol{q}^* = \{\boldsymbol{q}^*, \boldsymbol{\epsilon}^t \boldsymbol{\phi}\} = 0\,, \qquad \delta \boldsymbol{p}^* = \{\boldsymbol{p}^*, \boldsymbol{\epsilon}^t \boldsymbol{\phi}\} = \boldsymbol{\epsilon}^t \frac{\partial \boldsymbol{\phi}}{\partial \boldsymbol{q}}\,. \tag{31}$$

Arnold et al. [4] call any phase space function $F(\boldsymbol{q}^*, \boldsymbol{p}^*)$ which is invariant under this symmetry *observable*. Obviously, this implies that such an F contains $\boldsymbol{p}^*$ only in the form $\boldsymbol{p}^* - \boldsymbol{\lambda}^t \frac{\partial \boldsymbol{\phi}}{\partial \boldsymbol{q}}$ and that the Hamiltonian H^* is an example of an observable function. The symmetry can be easily understood. If we take two generating functions S with functions $\boldsymbol{\lambda}$ differing by *constants* $\boldsymbol{\epsilon}$, the resulting starred variables are related by the gauge transformation (31). But if the impetuses $\boldsymbol{p}^*$ appear only in the form $\boldsymbol{p}^* - \boldsymbol{\lambda}^t \frac{\partial \boldsymbol{\phi}}{\partial \boldsymbol{q}}$, the constants $\boldsymbol{\epsilon}$ drop out and we obtain identical results.

We can interpret this result also in another way. Basically it says that not the multipliers $\boldsymbol{\lambda}$ themselves are important but only their differentials, as we can add arbitrary constants. But this is not too surprising, if one compares again the two Lagrangians L' and L^*. We saw already that they are equivalent upon the identification $\boldsymbol{\mu} = -d\boldsymbol{\lambda}/dt$. Thus already here only the differentials of the multipliers $\boldsymbol{\lambda}$ plays a role.

6 Impetuses and Mass-Orthogonal Projections

The deeper meaning of the transformation (22) between the momenta and the impetuses becomes particularly clear for natural systems. Thus we assume now again that the configuration space $\mathcal{Q}$ is a Riemannian manifold. The metric induces a scalar product $\langle\cdot,\cdot\rangle_M$ on the phase space $T^*\mathcal{Q}$ which has the same form as the one on the tangent bundle $T\mathcal{Q}$ but now with the inverse mass matrix M^{-1}: $\langle \boldsymbol{u}, \boldsymbol{v}\rangle_M = \boldsymbol{u}^t M^{-1}\boldsymbol{v}$. The Hamiltonian of a natural system is then $H(\boldsymbol{q}, \boldsymbol{p}) = \frac{1}{2}\langle \boldsymbol{p}, \boldsymbol{p}\rangle_M + V(\boldsymbol{q})$ where again V denotes a real-valued potential. The use of the mass metric apparently goes back at least to Hertz. More recently it was studied in connection with constrained systems by Bayo and Ledesma [5] and by Brauchli [6].

If we impose on such a system position constraints $\boldsymbol{\phi}(\boldsymbol{q}) = 0$, then the corresponding momentum constraints may be written in the form $\boldsymbol{\psi}(\boldsymbol{q}, \boldsymbol{p}) = \left\langle \frac{\partial \boldsymbol{\phi}}{\partial \boldsymbol{q}}(\boldsymbol{q}), \boldsymbol{p}\right\rangle_M$ which implies that the strictions are determined by the *linear* system

$$\left\langle \frac{\partial \boldsymbol{\phi}}{\partial \boldsymbol{q}}(\boldsymbol{q}), \frac{\partial \boldsymbol{\phi}}{\partial \boldsymbol{q}}(\boldsymbol{q})\right\rangle_M \boldsymbol{\lambda} = \left\langle \frac{\partial \boldsymbol{\phi}}{\partial \boldsymbol{q}}(\boldsymbol{q}), \boldsymbol{p}^*\right\rangle_M = \boldsymbol{\psi}(\boldsymbol{q}, \boldsymbol{p}^*)\,. \tag{32}$$

The canonical transformation (24) with $\boldsymbol{\lambda}$ determined by (32) represents now for all points $(\boldsymbol{q}^*, \boldsymbol{p}^*) \in \mathcal{M}_1$, i. e. satisfying $\boldsymbol{\phi}(\boldsymbol{q}^*) = 0$, a mass-orthogonal projection on the secondary constraint manifold $\mathcal{M}_2$. Indeed, the transformation (24) simplifies to (26) for points on $\mathcal{M}_1$. For a given $\boldsymbol{q}$, the manifold $\mathcal{M}_2$ is a hyperplane whose Hesse normal form is defined by the vanishing of the momentum constraint functions. Thus we make the ansatz $\boldsymbol{p} = \boldsymbol{p}^* - \boldsymbol{\rho}^t \frac{\partial \boldsymbol{\phi}}{\partial \boldsymbol{q}}$ for a mass-orthogonal projection on $\mathcal{M}_2$. The multipliers $\boldsymbol{\rho}$ are uniquely determined by the condition $\boldsymbol{\psi}(\boldsymbol{q}, \boldsymbol{p}) = 0$. But this yields obviously the linear system (32) defining the strictions and hence the orthogonal projection is given by (26).

One can try to generalise this result to arbitrary Hamiltonian systems. Again one starts with a point $(\boldsymbol{q}^*, \boldsymbol{p}^*) \in \mathcal{M}_1$ and would like to find the point $(\boldsymbol{q}, \boldsymbol{p}) \in \mathcal{M}_2$ which has the minimal distance to $(\boldsymbol{q}^*, \boldsymbol{p}^*)$. However, only natural systems provide a canonical metric and thus a canonical way to measure distances. Furthermore, the momentum constraints $\boldsymbol{\psi}$ are generally nonlinear and we cannot use a simple projection to obtain $(\boldsymbol{q}, \boldsymbol{p})$. Hence it is not clear, how one could rigorously formulate a generalisation.

Taking a more operational point of view, one nevertheless obtains some sort of generalisation. We describe first a concrete method to compute a sequence of points $(\boldsymbol{q}, \boldsymbol{p}_k)$ which may be considered as approximating the "minimal" point $(\boldsymbol{q}, \boldsymbol{p})$. Then we show that we find exactly the same sequence of points, if we determine the strictions $\boldsymbol{\lambda}$ by a Newton iteration. In such a generalised sense one may consider the transformation (26) even for arbitrary Hamiltonian systems as a kind of orthogonal projection.

In order to approximate the "minimal point" $(\boldsymbol{q}, \boldsymbol{p})$ we take $\boldsymbol{q} = \boldsymbol{q}^*$ and must then solve the under-determined nonlinear system $\boldsymbol{\psi}(\boldsymbol{q}, \boldsymbol{p}) = 0$. This can be done using a Newton iteration with initial value $\boldsymbol{p}_0 = \boldsymbol{p}^*$. Writing $\boldsymbol{p}_{k+1} = \boldsymbol{p}_k - \mathbf{d}_k$ and noting that $\frac{\partial \boldsymbol{\psi}}{\partial \boldsymbol{p}} = \left(\frac{\partial \boldsymbol{\phi}}{\partial \boldsymbol{q}}\right)^t \frac{\partial^2 H}{\partial \boldsymbol{p} \partial \boldsymbol{p}}$, we obtain the following linear system for $\mathbf{d}_k$:

$$\left(\frac{\partial \boldsymbol{\phi}}{\partial \boldsymbol{q}}(\boldsymbol{q})\right)^t \frac{\partial^2 H}{\partial \boldsymbol{p} \partial \boldsymbol{p}}(\boldsymbol{q}, \boldsymbol{p}_k)\, \mathbf{d}_k = \boldsymbol{\psi}(\boldsymbol{q}, \boldsymbol{p}_k)\,. \tag{33}$$

Defining M as the inverse of the Hessian $\frac{\partial^2 H}{\partial \boldsymbol{p} \partial \boldsymbol{p}}$ evaluated at the point $(\boldsymbol{q}, \boldsymbol{p}_k)$, we again introduce a scalar product $\langle \cdot, \cdot \rangle_M$ and rewrite the linear system as

$$\left\langle \frac{\partial \boldsymbol{\phi}}{\partial \boldsymbol{q}}(\boldsymbol{q}), \mathbf{d}_k \right\rangle_M = \boldsymbol{\psi}(\boldsymbol{q}, \boldsymbol{p}_k)\,. \tag{34}$$

(34) is an under-determined system and does not possess a unique solution. Since we want to approximate the point $(\boldsymbol{q}, \boldsymbol{p})$ with "minimal distance" from $(\boldsymbol{q}^*, \boldsymbol{p}^*)$, we choose the solution that is minimal with respect to the mass norm. Alishenas [2] calls this the *M-minimal solution* and shows how it can be computed with the help of a pseudo-inverse: if $A\mathbf{x} = \mathbf{b}$ is an under-determined linear system, then its M-minimal solution is given by $A^- \mathbf{b}$ where $A^- = M^{-1} A^t (A M^{-1} A^t)^{-1}$ is the M-pseudo-inverse (for $M = I$ it is just the usual Moore-Penrose pseudo-inverse). The M-minimal solution of (34) is then

$$\mathbf{d}_k = \frac{\partial \boldsymbol{\phi}}{\partial \boldsymbol{q}} \left[\left(\frac{\partial \boldsymbol{\phi}}{\partial \boldsymbol{q}}\right)^t M \frac{\partial \boldsymbol{\phi}}{\partial \boldsymbol{q}} \right]^{-1} \boldsymbol{\psi}(\boldsymbol{q}, \boldsymbol{p}_k)\,. \tag{35}$$

In the impetus-striction formalism, we get the nonlinear system (25) for the strictions $\boldsymbol{\lambda}$. Again we use the Newton method to solve it, this time with the initial value $\boldsymbol{\lambda}_0 = 0$. The iteration takes the form

$$\boldsymbol{\lambda}_{k+1} = \boldsymbol{\lambda}_k - \left[\left(\frac{\partial \boldsymbol{\phi}}{\partial \boldsymbol{q}}\right)^t M \frac{\partial \boldsymbol{\phi}}{\partial \boldsymbol{q}} \right]^{-1} \boldsymbol{\psi}\Big(\boldsymbol{q}, \boldsymbol{p}^* - \boldsymbol{\lambda}_k^t \frac{\partial \boldsymbol{\phi}}{\partial \boldsymbol{q}}\Big) \tag{36}$$

where M is the inverse of the Hessian $\frac{\partial^2 H}{\partial \boldsymbol{p} \partial \boldsymbol{p}}$ evaluated at $\big(\boldsymbol{q}, \boldsymbol{p}^* - \boldsymbol{\lambda}_k^t \frac{\partial \boldsymbol{\phi}}{\partial \boldsymbol{q}}\big)$. A comparison with (35) shows at once that the two approaches are equivalent and related by

$$\boldsymbol{p}_k = \boldsymbol{p}^* - \boldsymbol{\lambda}_k^t \frac{\partial \boldsymbol{\phi}}{\partial \boldsymbol{q}}\,, \qquad k = 0, 1, 2, \dots \tag{37}$$

7 Position Versus Momentum Projection

We turn now our attention to the problem of numerically computing the trajectories of a constrained Hamiltonian system. However, we will restrict our discussion to the case of a regular system over an N-dimensional configuration space with K externally imposed position constraints $\boldsymbol{\phi}(\boldsymbol{q}) = 0$ and the associated momentum constraints $\boldsymbol{\psi}(\boldsymbol{q}, \boldsymbol{p}) = 0$. As we have already seen, we have a wide choice for the formulation of the equations of motion.

The classical approach is based on the formulation (15). Analytically, it can be treated as follows: we solve (16) for $\boldsymbol{\mu}$, enter the result into (15), choose initial values satisfying *all* constraints and integrate the differential part of (15). Any such computed solution stays on the constraint manifold. The constraints are considered only when choosing the initial data. Numerically, this approach has two disadvantages. Firstly, the underlying equation obtained by entering the multipliers into (15) is not Hamiltonian. This excludes for example the use of symplectic integrators. Secondly, in contrast to the analytical solution, the numerical solution generally drifts off from the constraint manifold.

Projection methods are a popular cure against the drift off [13]. In their simplest form, following a step with an arbitrary integrator, one projects the computed point $(\tilde{\boldsymbol{q}}_n, \tilde{\boldsymbol{p}}_n)$ onto the constraint manifold to obtain the final approximation $(\boldsymbol{q}_n, \boldsymbol{p}_n)$. We may distinguish *position projections* where only $\tilde{\boldsymbol{q}}_n$ is modified so that $\boldsymbol{\phi}(\boldsymbol{q}_n) = 0$ and *momentum projections* where only $\tilde{\boldsymbol{p}}_n$ is changed so that $\boldsymbol{\psi}(\boldsymbol{q}_n, \boldsymbol{p}_n) = 0$ (with $\boldsymbol{q}_n = \tilde{\boldsymbol{q}}_n$).

We will show that momentum projections are not only cheaper than position projections, as they require only the solution of a linear system, but that they yield better results, too. The absolute values and the growth rates of all relevant errors (energy and constraint residuals) are smaller. In particular, the energy error is much less affected by momentum projections.

Our basic tool is the comparison of two different underlying Hamiltonian systems. As seen in Section 4, the differential part of the equations of motion (17) obtained with the total Hamiltonian H_t is Hamiltonian and differs from (15) only by terms proportional to the position constraints functions $\boldsymbol{\phi}$. By contrast, the Hamilton-Dirac equations (21) differ from (15) only by terms multiplied by the momentum constraints functions $\boldsymbol{\psi}$. If we apply the corresponding projections, it makes no difference[6] whether we integrate numerically (15) or the respective underlying Hamiltonian system. In order to compare the two kind of projections we must thus study the stability of the constraint manifold for the two formulations.

The key for the stability analysis is the introduction of adapted coordinates. The equations $\boldsymbol{\phi}(\boldsymbol{q}) = \boldsymbol{\zeta}$, $\psi(\boldsymbol{q}, \boldsymbol{p}) = \boldsymbol{\rho}$ define for arbitrary constants $\boldsymbol{\zeta}$, $\boldsymbol{\rho}$ a $2(N-K)$-dimensional submanifold $\mathcal{M}_{\boldsymbol{\zeta},\boldsymbol{\rho}}$ of the full phase space. Let $\boldsymbol{f}(\boldsymbol{\xi}, \boldsymbol{\zeta})$ be N functions such that $\boldsymbol{\phi}\big(\boldsymbol{f}(\boldsymbol{\xi}, \boldsymbol{\zeta})\big) = \boldsymbol{\zeta}$ and that the matrix $\begin{pmatrix} \partial \boldsymbol{f}/\partial \boldsymbol{\xi} \\ (\partial \boldsymbol{\phi}/\partial \boldsymbol{q})^t \end{pmatrix}$ is regular. Then the equations

$$\boldsymbol{q} = \boldsymbol{f}(\boldsymbol{\xi}, \boldsymbol{\zeta}) \,, \qquad \frac{\partial \boldsymbol{f}}{\partial \boldsymbol{\xi}} \boldsymbol{p} = \boldsymbol{\pi} \,, \qquad \left(\frac{\partial \boldsymbol{\phi}}{\partial \boldsymbol{q}}\right)^t \boldsymbol{p} = \boldsymbol{\rho} \tag{38}$$

implicitly define coordinates $(\boldsymbol{\xi}, \boldsymbol{\pi})$ on $\mathcal{M}_{\boldsymbol{\zeta},\boldsymbol{\rho}}$.

On the submanifold $\mathcal{M}_{\boldsymbol{\zeta},\boldsymbol{\rho}}$, we may consider (38) as implicitly defining a coordinate transformation $\Gamma_{\boldsymbol{\zeta},\boldsymbol{\rho}} : (\boldsymbol{q}, \boldsymbol{p}) \mapsto (\boldsymbol{\xi}, \boldsymbol{\pi})$. One can show [29] that $\Gamma_{\boldsymbol{\zeta},\boldsymbol{\rho}}$ is in fact canonical and that its generating function is $S(\boldsymbol{\xi}, \boldsymbol{p}) = \boldsymbol{f}(\boldsymbol{\xi}, \boldsymbol{\zeta})\boldsymbol{p}$. Any function $F(\boldsymbol{q}, \boldsymbol{p})$ on $\mathcal{M}_{\boldsymbol{\zeta},\boldsymbol{\rho}}$ can be transformed into a function $\tilde{F}(\boldsymbol{\xi}, \boldsymbol{\pi})$ satisfying $F = \tilde{F} \circ \Gamma_{\boldsymbol{\zeta},\boldsymbol{\rho}}$.

Let H be the Hamiltonian of a natural system where we assume for simplicity that its mass matrix M is the identity. Then the transformed Hamiltonian $\tilde{H}$ is given by

$$\tilde{H}(\boldsymbol{\xi}, \boldsymbol{\pi}) = \frac{1}{2}\boldsymbol{\pi}^t \left[\left(\frac{\partial \boldsymbol{f}}{\partial \boldsymbol{\xi}}\right)^t \frac{\partial \boldsymbol{f}}{\partial \boldsymbol{\xi}}\right]^{-1} \boldsymbol{\pi} + \frac{1}{2}\boldsymbol{\rho}^t \left[\frac{\partial \boldsymbol{\phi}}{\partial \boldsymbol{q}} \left(\frac{\partial \boldsymbol{\phi}}{\partial \boldsymbol{q}}\right)^t\right]^{-1} \boldsymbol{\rho} + V \circ \boldsymbol{f} \,, \tag{39}$$

as $(\partial \boldsymbol{\phi}/\partial \boldsymbol{q})(\partial \boldsymbol{f}/\partial \boldsymbol{\xi}) = 0$ by the definition of $\boldsymbol{f}$ and $\boldsymbol{p} = \begin{pmatrix} \partial \boldsymbol{f}/\partial \boldsymbol{\xi} \\ (\partial \boldsymbol{\phi}/\partial \boldsymbol{q})^t \end{pmatrix}^{-1} \begin{pmatrix} \boldsymbol{\pi} \\ \boldsymbol{\rho} \end{pmatrix}$ by (38).

[6] This holds strictly only, if we project each time before we evaluate the equations of motion which is usually not true. But in our experience we can neglect this small error.

We introduce *perturbed Hamiltonian state space forms* where $\boldsymbol{\zeta}$, $\boldsymbol{\rho}$ model the constraint residuals. For the Hamilton-Dirac equations (13) we get

$$\dot{\boldsymbol{\xi}} = \{\boldsymbol{\xi}, \tilde{H}\}\,, \qquad \dot{\boldsymbol{\pi}} = \{\boldsymbol{\pi}, \tilde{H}\}\,. \tag{40}$$

For (17) we must use $\tilde{H}_t = \tilde{H} + \tilde{\boldsymbol{\mu}}^t\boldsymbol{\zeta}$ leading to a different perturbed state space form. But the *unperturbed* state space forms obtained by setting $\boldsymbol{\zeta} = \boldsymbol{\rho} = 0$ are identical in both cases.

The position constraint residuals $\boldsymbol{\zeta}$ appear in $\tilde{H}$ only via the functions $\boldsymbol{f}$; in $\tilde{H}_t$ we get an extra term $\tilde{\boldsymbol{\mu}}^t\boldsymbol{\zeta}$. The momentum constraint residuals $\boldsymbol{\rho}$ appear in (39) also in form of an extra term, a quadratic form. Extra terms in the Hamiltonian lead to extra terms in the equations of motion which may change their qualitative properties profoundly. But if momentum projections are used, i. e. if $\boldsymbol{\rho} = 0$, no extra terms appear. We may refine the analysis by considering $\boldsymbol{\zeta}$, $\boldsymbol{\rho}$ as time-dependent. This does not change the canonical transformation $\Gamma_{\boldsymbol{\zeta},\boldsymbol{\rho}}$, but we must subtract from $\tilde{H}$ the time derivative of the generating function [14]

$$\frac{\partial S}{\partial t} = \dot{\boldsymbol{\zeta}}^t \frac{\partial \boldsymbol{f}}{\partial \boldsymbol{\zeta}} \boldsymbol{p}\,. \tag{41}$$

Applying $\Gamma_{\boldsymbol{\zeta},\boldsymbol{\rho}}$ with time-dependent residuals $\boldsymbol{\zeta}$, $\boldsymbol{\rho}$ to (17) or (13) yields differential equations for $\boldsymbol{\xi}$, $\boldsymbol{\pi}$, $\boldsymbol{\zeta}$, $\boldsymbol{\rho}$. Those for $\dot{\boldsymbol{\xi}}$ and $\dot{\boldsymbol{\pi}}$ are the corresponding state space form; those for $\dot{\boldsymbol{\zeta}}$, $\dot{\boldsymbol{\rho}}$ are in general not Hamiltonian. The origin $\boldsymbol{\zeta} = \boldsymbol{\rho} = 0$ is a fixed point for the latter equations and its stability determines the drift off from the constraint manifold.

For the Hamilton-Dirac equations (13) we know even without computations that $\dot{\boldsymbol{\zeta}} = \dot{\boldsymbol{\rho}} = 0$ because of our considerations at the end of Section 3. Based on this result, we can straightforwardly analyse the use of momentum projections in the numerical integration of the classical equations of motion (15). The dynamics do not lead to any growth of the constraint residuals. Following Alishenas [2, 3], we use a continuous model for the error propagation and assume that because of numerical errors $\dot{\boldsymbol{q}} = \{\boldsymbol{q}, H\}^* + \boldsymbol{\epsilon}(t)$ with $||\boldsymbol{\epsilon}(t)|| < \hat{\epsilon}$ in the integration interval. Then $\dot{\boldsymbol{\zeta}} = \boldsymbol{\epsilon}(t)$ and the position constraint residual can grow at most linearly.

For the other underlying Hamiltonian system (17) one cannot make such general statements. But the following simple argument for $K = 1$ shows that we must expect a worse behaviour. In the coordinates $(\boldsymbol{q}, \boldsymbol{p})$ the growth of the constraint residuals is determined by $\dot{\phi} = \{\phi, H_t\} = \{\phi, \mu\}\phi + \psi$ and $\dot{\psi} = \{\psi, H_t\} = \{\psi, \mu\}\phi$. Linearisation about the origin yields $\dot{\phi} = 2a\phi + \psi$, $\dot{\psi} = b\phi$ with some time-dependent coefficients a, b. The eigenvalues of this linear system are $a \pm \sqrt{a^2 + b}$ and thus the origin is (linearly) unstable in general. Assuming that because of position projections $\phi(t) \approx \phi_0 \ll 1$, we still find from the equation for $\dot{\psi}$ that already the dynamics lead to an at least linear growth of the momentum constraint residual even without taking error propagation into account.

The growth of the constraint residuals is only one aspect in a comparison of the two types of projections. Another important aspect is to what extent the projections respect the structure of the system. Geometric integrators [16] are of growing importance in the numerical integration of dynamical systems. In our context, the main question is whether the projections preserve the Hamiltonian nature of the problem.

In order to answer this question, we first recall from the last section that a mass-orthogonal momentum projection is a canonical transformation for natural systems. We further showed there that in a certain sense this observation remains true for arbitrary systems. By contrast, a non-trivial position projection is never canonical. All possible extensions of a point transformation $\boldsymbol{q} = \boldsymbol{F}(\boldsymbol{Q})$ to a canonical transformation in phase space can be described by generating functions of the form $S = \boldsymbol{F}^t(\boldsymbol{Q})\boldsymbol{p} + G(\boldsymbol{Q})$ with a scalar function G [8, §§105–108]. Hence the momenta transform according to $\boldsymbol{P} = (\partial \boldsymbol{F}/\partial \boldsymbol{Q})^t \boldsymbol{p} + \partial G/\partial \boldsymbol{Q}$ and they only remain unchanged, if $\partial \boldsymbol{F}/\partial \boldsymbol{Q}$ is the identity matrix and G vanishes.

This observation may be used as basis for the design of symplectic integrators for constrained Hamiltonian systems. Indeed, the composition methods of Reich [24] exploit the (restricted) canonical transformation (26). By intertwining a momentum projection with a step of the integrator, it is even possible to simulate a "canonical" position projection, so that the arising symplectic methods preserve both the position and the momentum constraints.

Momentum projections also behave favourably with respect to energy conservation. For an integration method of order r, the (local) constraint residuals are of order $O(h^{r+1})$ [17]. Thus we must expect in general that a projection changes the energy in this order. However, a mass-orthogonal momentum projection changes the energy only in $O(h^{2r+2})$. The reason for this effect lies in the fact that the projection may be considered as the flow of the Hamiltonian $H_{\boldsymbol{\lambda}} = \boldsymbol{\lambda}^t \boldsymbol{\phi}(\boldsymbol{q})$ given by $\boldsymbol{q}(t) = \boldsymbol{q}_0$, $\boldsymbol{p}(t) = \boldsymbol{p}_0 - t\big[(\partial \boldsymbol{\phi}/\partial \boldsymbol{q})(\boldsymbol{q}_0)\big]^t \boldsymbol{\lambda}$. The energy error is thus determined by the change of H along an integral curve of $H_{\boldsymbol{\lambda}}$. At $t = 1$ we obtain in first order $\Delta E \approx \dot{H} = \{H, H_{\boldsymbol{\lambda}}\} = -\boldsymbol{\lambda}^t \boldsymbol{\psi}$. In the last section we saw that $\boldsymbol{\lambda} = R^{-1}\boldsymbol{\psi}$ with $R = \big\langle (\partial \boldsymbol{\phi}/\partial \boldsymbol{q}), (\partial \boldsymbol{\phi}/\partial \boldsymbol{q}) \big\rangle_M$ and thus $\Delta E \approx \boldsymbol{\psi}^t R^{-1} \boldsymbol{\psi}$. As by assumption $\boldsymbol{\psi} = O(h^{r+1})$, the momentum projection changes the energy in $O(h^{2r+2})$.

8 The Planar Pendulum in Cartesian Coordinates

The planar pendulum in Cartesian coordinates represents a standard example of a constrained natural system. Its equations are so simple that all transformations used above can be explicitly determined. Furthermore, the state space form is easily obtained and can be used to compute reference solutions with high precision.

The planar pendulum is described by the regular Hamiltonian $H = \frac{1}{2}(p_x^2 + p_y^2) + y$. The position constraint is $\phi(x, y) = \frac{1}{2}(x^2 + y^2 - 1) = 0$ and time differentiation of it leads to the momentum constraint $\psi(x, y, p_x, p_y) = xp_x + yp_y = 0$. For the multiplier one obtains $\mu = (p_x^2 + p_y^2 - y)/(x^2 + y^2)$. The classical equations of motion (15) are

$$\dot{x} = p_x\,, \qquad \dot{y} = p_y\,, \qquad \dot{p}_x = -\mu x\,, \qquad \dot{p}_y = -\mu y - 1\,. \tag{42}$$

The underlying Hamiltonian system (17) defined by $H_t = H + \mu\phi$ is

$$\begin{aligned} \dot{x} &= p_x + \frac{2p_x}{x^2 + y^2}\,\phi\,, & \dot{y} &= p_y + \frac{2p_y}{x^2 + y^2}\,\phi\,, \\ \dot{p}_x &= -\mu x + \frac{2x\mu}{x^2 + y^2}\,\phi\,, & \dot{p}_y &= -\mu y - 1 + \frac{2y\mu + 1}{x^2 + y^2}\,\phi\,. \end{aligned} \tag{43}$$

The Dirac bracket is $\{F, G\}^* = \{F, G\} - \frac{1}{x^2+y^2}\big(\{F, \phi\}\{\psi, G\} - \{F, \psi\}\{\phi, G\}\big)$ and the Hamilton-Dirac equations (21) yield the underlying system

$$\begin{aligned} \dot{x} &= p_x - \frac{x}{x^2 + y^2}\,\psi\,, & \dot{y} &= p_y - \frac{y}{x^2 + y^2}\,\psi\,, \\ \dot{p}_x &= -\mu x + \frac{p_x}{x^2 + y^2}\,\psi\,, & \dot{p}_y &= -\mu y - 1 + \frac{p_y}{x^2 + y^2}\,\psi\,. \end{aligned} \tag{44}$$

Obviously, on the constraint manifold (42), (43) and (44) are identical.

The canonical transformation (38) can be written explicitly as

$$\Gamma_{\zeta,\rho}\,:\,\begin{cases} x=\sqrt{2\zeta+1}\sin\xi\,, & y=\sqrt{2\zeta+1}\cos\xi\,,\\ p_x=\dfrac{\pi\cos\xi+\rho\sin\xi}{\sqrt{2\zeta+1}}\,, & p_y=\dfrac{-\pi\sin\xi+\rho\cos\xi}{\sqrt{2\zeta+1}} \end{cases} \tag{45}$$

where ζ represents the position and ρ the momentum constraint residual. Obviously, it simply changes to polar coordinates. This yields for the transformed Hamiltonian

$$\tilde{H}(\xi,\pi)=\frac{1}{2}\frac{\pi^2+\rho^2}{2\zeta+1}+\sqrt{2\zeta+1}\cos\xi-\frac{\rho\dot{\zeta}}{2\zeta+1} \tag{46}$$

where the last term is the time derivative (41) of the generating function.

Notice that for this special system the extra terms in $\tilde{H}$ do not depend on the dynamical variables (ξ,π). Thus they affect only the energy error but do not lead to extra terms in the perturbed state space forms. These are for (43)

$$\dot{\xi}=\frac{(4\zeta+1)}{(2\zeta+1)^2}\pi\,,\qquad \dot{\pi}=\frac{\zeta+1}{\sqrt{2\zeta+1}}\sin\xi \tag{47}$$

and for the Hamilton-Dirac equations (44)

$$\dot{\xi}=\frac{1}{2\zeta+1}\pi\,,\qquad \dot{\pi}=\sqrt{2\zeta+1}\sin\xi\,. \tag{48}$$

Superficially seen, the formulation (43) seems preferable, as a Taylor expansion shows that the perturbations in (47) are $O(\zeta^2)$ whereas they are $O(\zeta)$ in (48). However, this point of view neglects the much more important issue of the *growth* of the constraint residuals ζ, ρ. As mentioned above, we have $\dot{\zeta}=\dot{\rho}=0$ for the Hamilton-Dirac equations of any system. Applying the canonical transformation (45) to (43) yields

$$\dot{\zeta}=\frac{4\zeta+1}{2\zeta+1}\rho\,,\qquad \dot{\rho}=4\frac{\zeta(\rho^2+\pi^2)}{(2\zeta+1)^2}-\frac{\zeta\cos\xi}{\sqrt{2\zeta+1}}\,. \tag{49}$$

The eigenvalues of the linearised system are $\pm\sigma$ with $\sigma=\sqrt{4\pi^2-\cos\xi}$. Thus whenever σ is real, the origin is unstable for (49).

Assuming that due to position projections $\zeta\approx\zeta_0\ll 1$, we obtain for the residual ρ the Riccati equation $\dot{\rho}=\zeta_0(\sigma^2+4\rho^2)$. For the initial data $\rho(0)=\rho_0$ it has the closed-form solution $\rho(t)=\frac{\sigma}{2}\tan\bigl[2\sigma\zeta_0 t+\arctan(\frac{2\rho_0}{\sigma})\bigr]\approx\rho_0+\zeta_0(\sigma^2+4\rho_0^2)t+O(\zeta_0^2t^2)$. Thus for small times t already the dynamics yield an at least linear growth of the momentum constraint residual. Note that this even holds, if $\rho_0=0$.

We integrated the classical equations of motion (42) for the initial data $(x^0,y^0,p_x^0,p_y^0)=(1,0,0,-2)$ until $t=1023$ with the standard fourth-order Runge-Kutta method using the step size $h=0.025$. For these data the pendulum rotates clockwise with the period $T=3.31$. We projected, when the corresponding residual exceeded $\epsilon=10^{-6}$. Fig. 1 (upper part) shows the integration error (estimated by comparing with an integration of the state-space form with step size $h/10$) without (`w/o`), with momentum (`mom`) and with position projections (`pos`).

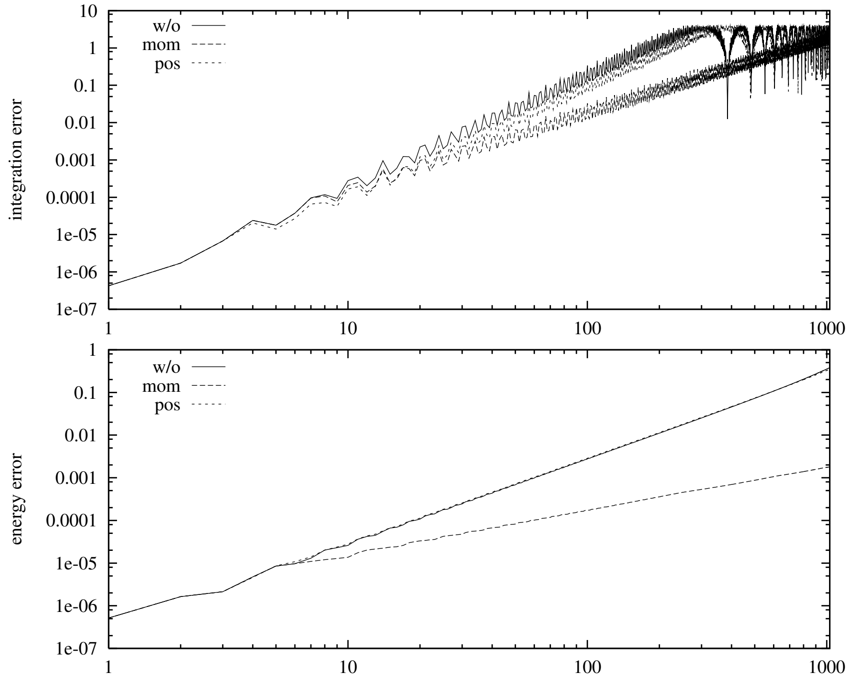

Fig. 1 Integration and energy error for the planar pendulum

Position projections hardly improve the results. They yield the same energy error as without, whereas momentum projections significantly reduce it (Fig. 1, lower part). Furthermore, they have no effect on the momentum constraint residual. In contrast, momentum projections improve the position constraint residual by more than two orders of magnitude compared to without projections. In the end it is $5 \cdot 10^{-4}$.

Momentum projections also yield smaller error *growth rates*. Without projections the integration error grows cubically, the energy error and the position constraint residual quadratically and the momentum constraint residual linearly. These rates are not changed by position projections. Momentum projections lead to a quadratic growth of the integration error and a linear growth of energy error and position constraint residual.

These observations can be partially explained by our results in the last section where e. g. the linear growth of the remaining residual after projection on one constraint was predicted. The growth rates of the energy errors come from the perturbed Hamiltonian $\tilde{H}$. The momentum constraint residual ρ grows linearly after position projections. As it appears quadratically in (46), we expect an at least quadratic growth of the energy error. For the error after momentum projections the dependency of $\tilde{H}$ on the position constraint residual ζ is decisive. The series expansion contains a linear term that dominates the higher order terms because of the smallness of ζ in our integration interval. As ζ grows linearly, so does the energy error.

In order to check the periodicity of the solutions we computed a periodogram from the values at $t = 0, 1, 2, \ldots, 1023$. With momentum projections it hardly differs from the one obtained from the state space form and consists essentially of one spike at $f = 0.302$ with amplitude 0.39. Since $f = 1/T$, the periodicity is very well maintained. Without projections the spike is smeared over the range 0.3–0.37 with a maximal amplitude of 0.05. Position projections yield only a small improvement.

The most striking result is that these considerable improvements have been achieved with only 155 momentum projections, i. e. on average after 260 integration steps. In contrast, position projections were needed after almost every step. With a tighter error tolerance the results for momentum projections further improve, whereas this makes hardly any difference for position projections. With $\epsilon = 10^{-8}$ one needs on average after 3 integration steps a momentum projection, the maximal value of the integration error is about $3 \cdot 10^{-3}$, of the energy error $3 \cdot 10^{-5}$ and of the position constraint residual 10^{-5}.

Other numerical methods yield similar results. Hairer and Wanner [17, p. 472] applied the Dormand-Prince 5(4) pair to the pendulum and observed that the integration error became even worse, when position projections were used. They also noted that adding position projections to momentum projections hardly changes the results.

For deriving the impetus-striction formulation of the planar pendulum, we first need the striction. It is easily determined to be $\lambda = (x^* p_x^* + y^* p_y^*)/\big((x^*)^2 + (y^*)^2\big)$. The arising equations of motion are then

$$\dot{x}^* = p_x\,, \qquad \dot{y}^* = p_y\,, \qquad \dot{p}_x^* = \lambda p_x\,, \qquad \dot{p}_y^* = \lambda p_y - 1 \tag{50}$$

where $p_x = p_x^* - \lambda x^*$ and $p_y = p_y^* - \lambda y^*$ are the classical momenta. We do not present an error plot for their numerical integration, as the results are similar to those obtained above with momentum projections. Indeed, as discussed in Section 6, the classical momenta are just the projected impetuses. Note however that if we use (50), then we perform these projections at each evaluation of the right hand side whereas we have seen above that in the numerical integration of (42) fairly few projections were necessary. Hence from a computational point of view the latter approach seems preferable.

We use the impetus-striction formulation to study numerically the stability of the constraint manifold. The manifolds $\mathcal{M}_\epsilon$ are concentric circles in the x^*–y^* plane and for any initial data (x^0, y^0, p_x^0, p_y^0) the projection of the solution of the impetus-striction equations (50) on this plane is just the corresponding circle. In numerical experiments the orbital stability can be well observed; the left part of Fig. 2 shows the x^*–y^* phase portrait for the exact initial data used above and for slightly perturbed initial data $(x^0, y^0, p_x^0, p_y^0) = (1.1, 0.1, 0.1, -1.9)$; note that we start here with inconsistent momentum values.

Sofer et al. [33] compared numerically several formulations of the equations of motions for the planar pendulum. Their formulation C corresponds to the impetus-striction formalism. They showed that the linearisation of the corresponding equations of motion about the periodic solution on the constraint manifold has an unstable direction. More precisely, the eigenvalues at a point P on the orbit are 0 (algebraically double and geometrically simple) and $\pm\lambda$ where λ is the value of the striction at P.

However, one must be careful with the linear stability analysis of a Hamiltonian system, as critical elements are here rarely hyperbolic. In numerical experiments one indeed observes an instability in the impetuses. Their phase portrait shows an outward going spiral (see the right part of Fig. 2). But this effect seems to be more related to the double eigenvalue 0 than to the pair of real eigenvalues: the growth of the amplitude is only linear and the p_x^*- and p_y^*-components of the eigenvector to 0 are proportional to x^* and y^*, respectively, i. e. they point

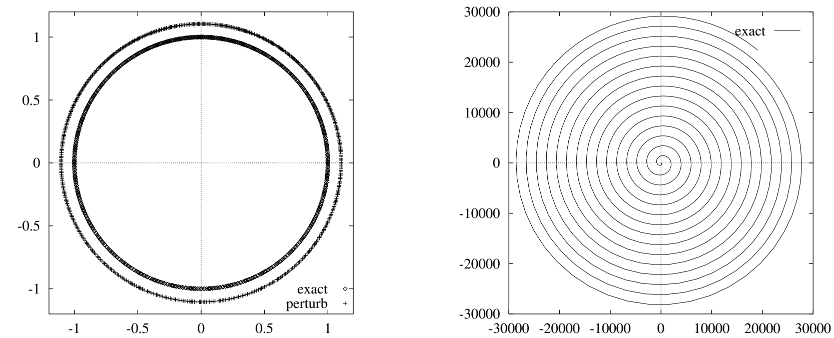

Fig. 2 Phase portraits for the planar pendulum (left x^*-y^*, right p_x^*-p_y^*)

in radial direction (normal to the constraint manifold). Also no observable like the energy or the physical momenta p_x, p_y shows an instability: the observed instability of the impetuses is eliminated by the radial projection relating the impetuses p_x^*, p_y^* with p_x, p_y.

Analytically the instability of the normal part of the impetus vector can be easily derived for this simple system. If we compute its time derivative, we obtain

$$\frac{d}{dt}(x^* p_x^* + y^* p_y^*) = \frac{(x^* p_y^* - y^* p_x^*)^2}{(x^*)^2 + (y^*)^2} - y^* \, . \tag{51}$$

The denominator of the first term is an integral of motion and thus constant along any trajectory. The numerator is the square of the angular momentum (one easily checks that here $xp_y - yp_x = x^* p_y^* - y^* p_x^*$). If we had taken the pendulum without gravitation, the y^*-term would be missing and the angular momentum would be another integral of motion. Hence without gravitation the time derivative would be constant and we would get an exact linear growth. In our case we have $\frac{d}{dt}(x^* p_y^* - y^* p_x^*) = -x^*$. But if we average over one period, $\langle x^* \rangle = 0$ and similarly for the y^*-term in (51). Thus the average growth of the normal part of the impetus vector is indeed linear as observed.

In our example this growth of the normal part of the impetus vector caused no problems. In general we must, however, expect a loss of numerical precision. As this normal part is the right hand side of (32), the strictions also grow linearly. In the projection relating $\boldsymbol{p}$ and $\boldsymbol{p}^*$ we must then compute the small difference between two large vectors. In larger examples one can indeed observe a slow degradation of the results due to this effect.

Fortunately, there exists a simple cure for this problem. We mentioned already above that we can choose the initial value of the strictions arbitrarily, as two different values are related by the gauge transformation (31). We are free to apply such a transformation at any time. If after some time the amplitude of the impetuses is too large, we simply "reset" them: $p_x^* \leftarrow p_x^* - \lambda x$ and $p_y^* \leftarrow p_y^* - \lambda y$. This will not effect any of the physical observables. This strategy was already employed by Ruhoff et al. [25] in their simulations of pendulum chains. They report that for larger chains they had to perform momentum projections in order to obtain reasonable results. But these projections are of course equivalent to our "resetting" of the impetuses.

The pair of real eigenvalues $\pm\lambda$ is probably only an artifact of the linearisation. The mass-orthogonal projection which forms the core of the impetus-striction formalism is non-linear and thus destroyed by the linearisation. If we consider the striction as a constant, we can see the origin of these eigenvalues in the equations of motion (50): the equations for $\dot{x}^*$ and $\dot{y}^*$ contain terms $-\lambda x^*$ and $-\lambda y^*$, respectively, and those for $\dot{p_x}^*$ and $\dot{p_y}^*$ terms λp_x^* and λp_y^*, respectively. But this linear point of view neglects that these terms always appear as parts of the combinations $p_x^* - \lambda x^*$ and $p_y^* - \lambda y^*$, respectively. Thus we may assume that the real eigenvalues are irrelevant for the nonlinear stability analysis.

In the example of the planar pendulum, the instability can also be considerably damped with a simple trick. The Hamiltonian of a constrained system is well-defined only *on* the constraint manifold; we may add an arbitrary linear combination of the constraint functions without changing the dynamics. We use this freedom and take the Hamiltonian

$$\bar{H} = \frac{1}{2}(x^2 + y^2)(p_x^2 + p_y^2) + y\,. \tag{52}$$

Obviously, H and $\bar{H}$ coincide when $x^2 + y^2 = 1$. With $\nu = x^* p_y^* - y^* p_x^*$ this modified Hamiltonian yields as impetus-striction equations of motion

$$\dot{x}^* = -\nu y^*\,, \qquad \dot{y}^* = \nu x^*\,, \qquad \dot{p_x}^* = -\nu p_y^*\,, \qquad \dot{p_y}^* = \nu p_x^* - 1\,. \tag{53}$$

In linear analysis this system is stable, as its eigenvalues ($\pm i\nu$ and $\pm\sqrt{3}i\nu$) are purely imaginary. However, the system is still nonlinearly unstable, as one observes qualitatively the same picture as in the right part of Fig. 2. But with the same parameters as before, one obtains a much smaller maximal amplitude of about 1000 compared with about 30000 for (50).

One should note that the classical equations of motion (42) are unstable, too. Evaluation of the eigenvalues of its linearisation of the constraint manifold yields $\pm\sqrt{p_x^2 + p_y^2}$ and $\pm i\sqrt{p_x^2 + p_y^2 - y}$. Thus there also exist unstable directions which lead to the well-known drift off the constraint manifold. Sofer et al. [33] presented two formulations of the pendulum which are linearly stable. However, none of them is Hamiltonian in contrast to (53).

References

[1] R. Abraham and J.E. Marsden. *Foundations of Mechanics*. Benjamin-Cummings, Reading, 2^{nd} edition, 1978.

[2] T. Alishenas. *Zur Numerischen Behandlung, Stabilisierung durch Projektion und Modellierung Mechanischer Systeme mit Nebenbedingungen und Invarianten*. PhD thesis, Dept. of Numerical Analysis and Computer Science, Royal Institute of Technology, Stockholm, Sweden, 1992.

[3] T. Alishenas and Ö. Ólafsson. Modeling and velocity stabilization of constrained mechanical systems. *BIT*, 34:455–483, 1994.

[4] V.I. Arnold, V.V. Kozlov, and A.I. Neishtadt. Mathematical aspects of classical and celestial mechanics. In V.I. Arnold, editor, *Dynamical Systems III*. Springer-Verlag, Berlin, 1988.

[5] E. Bayo and R. Ledesma. Augmented Lagrangian and mass-orthogonal projection methods for constrained multibody dynamics. *Nonl. Dyn.*, 9:113–130, 1996.

[6] H. Brauchli. Mass-orthogonal formulation of equations of motion for multibody systems. *ZAMP*, 42:169–182, 1991.

[7] K.E. Brenan, S.L. Campbell, and L.R. Petzold. *Numerical Solution of Initial-Value Problems in Differential-Algebraic Equations*. Classics in Applied Mathematics 14. SIAM, Philadelphia, 1996.

[8] C. Carathéodory. *Variationsrechnung und Partielle Differentialgleichungen erster Ordnung, Band I*. Teubner, Leipzig, 1956.

[9] D.J. Dichmann and J.H. Maddocks. An impetus-striction simulation of the dynamics of an elastica. *J. Nonlin. Sci.*, 6:271–292, 1996.
[10] D.J. Dichmann, J.H. Maddocks, and R.L. Pego. Hamiltonian dynamics of an elastica and the stability of solitary waves. *Arch. Rat. Mech. Anal.*, 135:357–396, 1996.
[11] P.A.M. Dirac. Generalized Hamiltonian dynamics. *Can. J. Math.*, 2:129–148, 1950.
[12] P.A.M. Dirac. Generalized Hamiltonian dynamics. *Proc. Roy. Soc. A*, 246:326–332, 1958.
[13] E. Eich, C. Führer, B. Leimkuhler, and S. Reich. Stabilization and projection methods for multibody dynamics. Research Report A281, Helsinki University of Technology, Institute of Mathematics, 1990.
[14] H. Goldstein. *Classical Mechanics*. Addison-Wesley, New York, 1980.
[15] W. Hahn. *Stability of Motion*. Grundlehren der mathematischen Wissenschaften 138. Springer-Verlag, Berlin, 1967.
[16] E. Hairer, C. Lubich, and G. Wanner. *Geometric Numerical Integration. Structure Preserving Algorithms for Ordinary Differential Equations*. Springer Series in Computational Mathematics 31. Springer-Verlag, Berlin, 2002.
[17] E. Hairer and G. Wanner. *Solving Ordinary Differential Equations II*. Springer Series in Computational Mathematics 14. Springer-Verlag, Berlin, 1996.
[18] M. Henneaux and C. Teitelboim. *Quantization of Gauge Systems*. Princeton University Press, 1992.
[19] S.W. de Leeuw, J.W. Perram, and H.G. Petersen. Hamilton's equations for constrained dynamical systems. *J. Stat. Phys.*, 61:1203–1222, 1990.
[20] B.J. Leimkuhler and S. Reich. Symplectic integration of constrained Hamiltonian systems. *Math. Comp.*, 63:589–605, 1994.
[21] A.D. Lewis and R.M. Murray. Variational principles for constrained systems: Theory and experiments. *Int. J. Non-lin. Mech.*, 30:793–815, 1995.
[22] J.H. Maddocks and R.L. Pego. An unconstrained Hamiltonian formulation for incompressible fluid flow. *Comm. Math. Phys.*, 170:207–217, 1995.
[23] P.J. Rabier and W.C. Rheinboldt. Theoretical and numerical analysis of differential-algebraic equations. In P.G. Ciarlet and J.L. Lions, editors, *Handbook of Numerical Analysis*, volume VIII, pages 183–540. North-Holland, Amsterdam, 2003.
[24] S. Reich. Symplectic integration of constrained Hamiltonian systems by composition methods. *SIAM J. Num. Anal.*, 33:475–491, 1996.
[25] P.T. Ruhoff, E. Præstgaard, and J.W. Perram. Efficient algorithms for simulating complex mechanical systems using constraint dynamics. *Proc. Roy. Soc. Lond. A*, 452:1139–1165, 1996.
[26] J.M. Sanz-Serna and M.P. Calvo. *Numerical Hamiltonian Problems*. Applied Mathematics and Mathematical Computation 7. Chapman & Hall, London, 1994.
[27] A.J. van der Schaft and B.M. Maschke. On the Hamiltonian formulation of nonholonomic mechanics systems. *Rep. Math. Phys.*, 34:225–233, 1994.
[28] W.M. Seiler. Impetus-striction formalism and the numerical integration of constrained Hamiltonian systems. In preparation.
[29] W.M. Seiler. Momentum versus position projections for constrained Hamiltonian systems. *Num. Algo.*, 19:223–234, 1998.
[30] W.M. Seiler. Numerical analysis of constrained Hamiltonian systems and the formal theory of differential equations. *Math. Comp. Simul.*, 45:561–576, 1998.
[31] W.M. Seiler. Numerical integration of constrained Hamiltonian systems using Dirac brackets. *Math. Comp.*, 68:661–681, 1999.
[32] W.M. Seiler and R.W. Tucker. Involution and constrained dynamics I: The Dirac approach. *J. Phys. A: Math. Gen.*, 28:4431–4451, 1995.
[33] M. Sofer, O. Melliger, and H. Brauchli. Numerical behaviour of different formulations for multibody dynamics. In Ch. Hirsch, O.C. Zienkiewicz, and E. Oñate, editors, *Numerical Methods in Engineering '92*, pages 277–284. Elsevier, Amsterdam, 1992.